Incorporating the Effect of Ionic Strength in Free Energy Calculations Using Explicit Ions

SERENA DONNINI,[1] ALAN E. MARK,[2] ANDRÉ H. JUFFER,[1] ALESSANDRA VILLA[2]
[1]*The Biocenter and the Department of Biochemistry, University of Oulu, P.O. Box 3000 ,FIN-90014, University of Oulu, Finland*
[2]*Groningen Biomolecular Sciences and Biotechnology Institute (GBB), Department of Biophysical Chemistry, University of Groningen, Nijenborgh 4, 9747 AG Groningen, The Netherlands*

Received 10 May 2004; Accepted 20 August 2004
DOI 10.1002/jcc.20156
Published online in Wiley InterScience (www.interscience.wiley.com).

Abstract: The incorporation of explicit ions to mimic the effect of ionic strength or to neutralize the overall charge on a system in free energy calculations using molecular dynamics simulations is investigated. The difference in the free energy of hydration between two triosephosphate isomerase inhibitors calculated at five different ion concentrations is used as an example. We show that the free energy difference can be highly sensitive to the presence of explicit ions even in cases where the mutation itself does not involve a change in the overall charge. The effect is most significant if the molecule carries a net charge close to the site mutated. Furthermore, it is shown that the introduction of a small number of ions can lead to very severe sampling problems suggesting that in practical calculations convergence can best be achieved by incorporating either no counterions or by simulating at high ionic strength to ensure sufficient sampling of the ion distribution.

 J Comput Chem 26: 115–122, 2005

Key words: molecular dynamics simulations; thermodynamic integration; free energy; ionic strength; triosephosphate isomerase inhibitors

Introduction

Advances in the field of computational chemistry have paved the way for calculating free energy differences associated with various chemical processes. Among others, these include the recognition of a ligand by a receptor and the solvation of a molecule. One common and theoretically rigorous method to estimate the difference in the free energy between two states of a system is the coupling parameter approach in conjunction with molecular dynamics (MD) simulation techniques using either the thermodynamic integration (TI) or thermodynamic perturbation formula.[1–4]

A recurring question in such calculations is the treatment of the solvent environment, and in particular, the treatment of ionic interactions. In many applications of free energy calculations to biomolecular systems[2,5] the ionic strength of the system has been ignored for reasons of efficiency. However, in the case of ligand–protein interactions, for example, this could easily result in erroneous estimates of the binding affinity as the chemicophysical environment is not described appropriately. Under physiological conditions large numbers of positive and negative ions are always present and the ionic strength of the environment is known to affect thermodynamic properties of a system, such as binding affinities[6,7] and thermal stability.[8] Although this effect is generally expected to be small, it can be as much as a few kJ mol^{-1} for a twofold increase in ionic strength in some cases and a significant ionic strength dependence is expected for bimolecular reactions involving charged species.[6,7]

The question of the incorporation of ions in free energy calculations is also important in systems where the solute carries a net charge. In such cases it is common practice to maintain the overall neutrality of the system by adding ions to compensate for the net charge of the solute to the simulation box. This, however, can lead to inconsistencies in the calculations. For example, when computing the free energy of binding of a neutral ligand to a charged protein, the charge on the protein may be compensated by counterions, while no ions might be included in the mutation involving the free ligand in water.[9] In such cases, it is unclear to what extent the ions, which were present in the simulation of the protein–ligand complex, but not in the simulation of the free ligand, could

Correspondence to: A. Villa; e-mail: A.Villa@chem.rug.nl

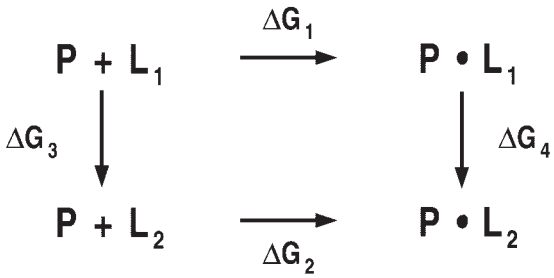

$$\Delta\Delta G = \Delta G_2 - \Delta G_1 = \Delta G_4 - \Delta G_3$$

Figure 1. Thermodynamic cycle for the calculation of relative free energy of binding, $\Delta\Delta G$, of ligands L_1 and L_2 to a protein P. ΔG_1 and ΔG_2 are the free energies of binding of L_1 and L_2 to P, respectively, and ΔG_3 and ΔG_4 are the free energy differences of L_1 and L_2 in water and in the binding pocket of the solvated protein P, respectively.

effect the overall free energy difference within the context of a thermodynamic cycle, as illustrated in Figure 1.

In addition, if the total charge of a molecule changes during the transformation the number of counterions must also change if overall neutrality is to be maintained. For example, if a charged ligand is mutated within the protein binding pocket, should one compensate for the change in overall charge by simultaneously adding/removing one or more ions from the system?[10] A consequence of such an approach is that one obtains the free energy of a combined process, namely the association of the ligand and the solvation of the ion.[11]

Here, we investigate the effect of ionic strength on the change in the free energy of hydration associated with a very simple mutation in a neutral and charged solute. The aim of the work is to demonstrate what effect the explicit incorporation of ions can have on the free energy one computes and on the convergence properties of the calculations. The mutation studied was the conversion of 2-phosphoglycolic acid into 3-phosphonopropanoic acid (Fig. 2), both of which are inhibitors of the enzyme triosephosphate isomerase (TIM).[12–14] The free energy difference was computed at five different ionic strengths: 0, 0.04, 0.06, 0.1, and 2 M. To compare the effect of the inclusion of ions on neutral and charged species, both the neutral and ionic ($-3e$) forms of the acids were considered.

Methods

The difference in the free energy of hydration between the two triosephosphate isomerase inhibitors, 2-phosphoglycolic acid and 3-phosphonopropanoic acid, was investigated with different concentrations of Na^+ and Cl^- ions (see Fig. 2). Calculations were performed on both the neutral and ionic ($-3e$) forms of the compounds. We refer to the neutral forms of 2-phosphoglycolic acid and 3-phosphonopropanoic acid as PGAH and 3PPH, respectively, and to the charged forms as PGA and 3PP, respectively. The GROMOS96 force field[15] was used to describe the compounds and the ions where possible. Aliphatic hydrogen atoms were treated as united atoms, together with the carbon atom to which they were attached. Force field parameters for the phosphate and phosphonate moiety of the inhibitors were derived from the force field parameters of phosphoserine.[16,17] Quantum mechanical calculations were performed with Gaussian94 program[18] to obtain an estimate of the charge distribution. The geometries of the four inhibitor molecules were optimized *in vacuo* at the RHF/6-31G(d) level of theory and the Mulliken charges of the optimized structures were determined. 1–4 interactions involving hydrogen atoms Hp1 and Hp2 (Fig. 2) were excluded. The partial

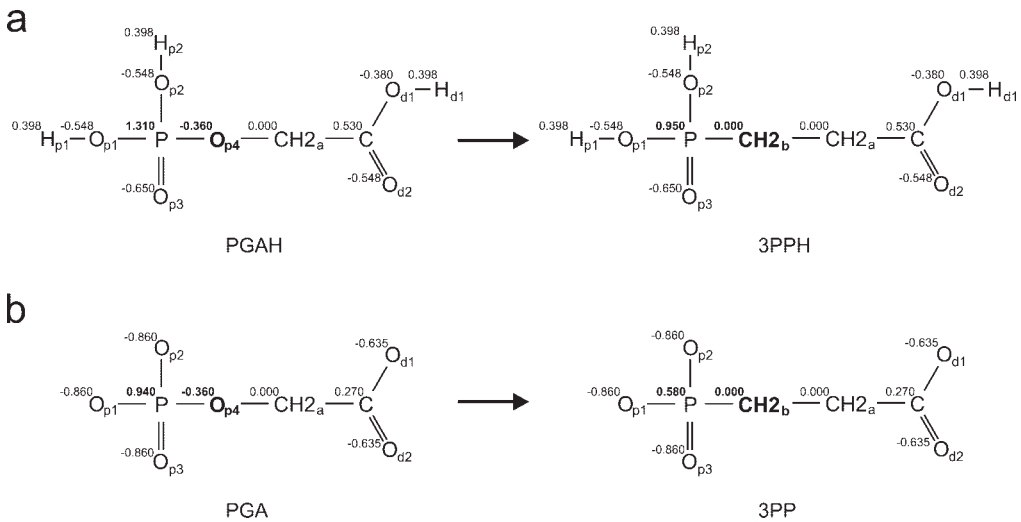

Figure 2. (a) Mutation of the neutral forms of 2-phosphoglycolic acid (PGAH) and 3-phosphonopropanoic acid (3PPH). (b) Mutation of the ionic forms of 2-phosphoglycolic acid (PGA) and 3-phosphonopropanoic acid (3PP). Atomic charges (e) are indicated in the upper left corner of each atom. The atom and charges that change in the mutation are indicated in bold.

Table 1. Bonded Parameters[a] Used for 2-Phosphoglycolic Acid and 3-Phosphonopropanoic Acid.

	PGAH/PGA			3PPH/3PP		
Bonds	b_0 (nm)	k^b (kJ mol^{-1} nm^{-4})		b_0 (nm)	k^b (kJ mol^{-1} nm^{-4})	
C-Od1 (PGAH/3PPH)	0.136	1.02e+07				
C-Od2 (PGAH/3PPH)	0.123	1.66e+07				
C-Od1/Od2 (PGA/3PP)	0.125	1.34e+07				
C-$CH2_a$	0.153	7.15e+06				
$CH2_a$-Op4/$CH2_b$	0.143	8.18e+06		0.153	7.15e+06	
Op4/$CH2_b$-P	0.161	4.84e+06		0.1797	4.84e+06	
P-Op1/Op2/Op3	0.148	8.60e+06				
Ox-Hx	0.100	1.57e+07				
Angles	θ_0 (Degree)	k^θ (kJ mol^{-1})		θ_0 (Degree)	k^θ (kJ mol^{-1})	
Od1-C-Od2 (PGAH/3PPH)	124.0	730.				
Od1-C-Od2 (PGA/3PP)	126.0	770.				
Od1-C-$CH2_a$ (PGAH/3PPH)	115.0	610.				
Od2-C-$CH2_a$ (PGAH/3PPH)	121.0	685.				
Od1/Od2-C-$CH2_a$ (PGA/3PP)	117.0	635.				
C-$CH2_a$-Op4/$CH2_b$	109.5	520.				
$CH2_a$-Op4/$CH2_b$-P	120.0	530.		113.0	545.	
Op4/$CH2_b$-P-Op3 (PGAH/3PPH)	109.6	450.				
Op4/$CH2_b$-P-Op1/Op2 (PGAH/3PPH)	103.0	420.				
Op4/$CH2_b$-P-Op1/Op2/Op3 (PGA/3PP)	109.6	450.				
Op1-P-Op2/Op3 (PGAH/3PPH)	109.6	450.				
Op2-P-Op3 (PGAH/3PPH)	109.6	450.				
Op1-P-Op2/Op3 (PGA/3PP)	120.0	780.				
Op2-P-Op3 (PGA/3PP)	120.0	780.				
Hx-Ox-X	109.5	450.				
Proper dihedrals	ϕ_0 (Degree)	k^ϕ (kJ mol^{-1})	n	ϕ_0 (Degree)	k^ϕ (kJ mol^{-1})	n
Od1-C-$CH2_a$-Op4/$CH2_b$	0.0	1.00	6			
C-$CH2_a$-Op4/$CH2_b$-P	0.0	3.77	3	0.0	5.86	3
$CH2_a$-Op4/$CH2_b$-P-Op1	0.0	1.05	3	0.0	2.93	3
Hd1-Od1-C-$CH2_a$	180.0	16.70	2			
Hpx-Opx-P-Op4	0.0	1.05	3			
Improper dihedrals	ε_0 (Degree)	k^ε (kJ mol^{-1} Degree^{-2})		ε_0 (Degree)	k^ε (kJ mol^{-1} Degree^{-2})	
C-Od1-Od2-$CH2_a$	0.0	0.051				

Parameters are for both neutral and charged forms (PGAH/PGA, 3PPH/3PP), unless indicated differently. For 3-phosphonopropanoic (3PPH/3PP), only the parameters modified during the mutation are reported explicitly. Atoms labeled according to Figure 2. The symbol "x" indicates any atom or index

[a]Bonded potential energy functions: bond potential: $V_b(b) = \frac{1}{4}k^b(b^2 - b_0^2)^2$; angle potential: $V_a(\theta) = \frac{1}{2}k^\theta(\cos\theta - \cos\theta_0)^2$; dihedral potential: $V_d(\phi) = k^\phi(1 + \cos(n\phi - \phi_0))$; improper dihedral potential: $V_{id}(\varepsilon) = \frac{1}{2}k^\varepsilon(\varepsilon - \varepsilon_0)^2$.

atomic charges and the bonded parameters are reported in Figure 2 and Table 1, respectively.

All molecular dynamics (MD) simulations were performed with the GROMACS suite of programs[19−21] (version 3.1). The inhibitors were placed in a cubic box (edge length approximately 4 nm), which was subsequently filled with ∼2170 SPC (Simple Point Charge) water molecules.[22] The calculations were performed at five different ionic strengths: 0, 0.04, 0.06, ∼0.1, and ∼2 M. These values refer to the ionic strength of the ion solution not including the solute. For the neutral forms (PGAH and 3PPH) simulations where performed including no ions, 3 Na^+, 4 Na^+ and 1 Cl^-, 4 Na^+ and 4 Cl^-, 79 Na^+ and 79 Cl^- ions. For the charged inhibitors (PGA and 3PP) simulations where performed with no ions, 3 Na^+, 4 Na^+ and 1 Cl^-, 6 Na^+ and 3 Cl^-, 80 Na^+ and 77 Cl^- ions. Note, at ionic strengths 0.1 and 2 M the number of ions in the charged and neutral systems are slightly different. This was done to maintain the overall neutrality of the system at higher ionic strengths. The ions were placed randomly in the simulation box. A twin range cutoff was used for the Coulomb and Lennard–Jones interactions. Interactions between atoms within 0.9 nm were evaluated every step, while interactions between atoms within 1.4 nm were evaluated every five steps. To correct for the neglect of

electrostatic interactions beyond the longer range cutoff, a reaction field (RF) correction with $\varepsilon_{RF} = 78.0$ was used. Constant pressure p and temperature T were maintained by weakly coupling the system to an external bath at 1 bar and 298 K using the Berendsen barostat and thermostat.[23] The inhibitor, the ions and the solvent were independently coupled to the temperature bath with a coupling time of 0.1 ps. The pressure coupling time was 1.0 ps and the isothermal compressibility $4.6 \cdot 10^{-5}$ bar^{-1}. A leap-frog integrator was used. The bond distances and the bond angle of water were constrained using the SETTLE algorithm.[24] All other bond distances were constrained using the LINCS algorithm.[25] The integration time step was 2 fs. Prior to the simulations, the potential energy of each system was minimized using a steepest descent approach, followed by a 10 ps MD simulation with position restraints on the inhibitor to relax the waters. Then, a 200 ps simulation was performed to equilibrate each system before initiating the free energy calculations.

To be able to estimate hydration free energies calculations were performed in vacuum using the same conditions as for the calculations in water. Note, in these calculations a reaction field with $\varepsilon_{RF} = 78.0$ was used beyond the 1.4 nm cutoff. This is necessary due to the specific implementation of the reaction field, which induces a fixed offset in the energy.

Free Energy Calculations

The free energy difference was estimated using the thermodynamic integration formula

$$\Delta G_{AB} = \int_{\lambda_A}^{\lambda_B} d\lambda \left\langle \frac{\partial H(\lambda)}{\partial \lambda} \right\rangle_{\lambda}, \quad (1)$$

where λ is a coupling parameter and H is the (classical) Hamiltonian of the system. The $\langle \partial H/\partial \lambda \rangle$ was estimated as the average $\partial H/\partial \lambda$ during the molecular dynamics simulation with λ kept constant. In total, 18 independent simulations were performed with different λ values between 0 to 1 to model the transformation of PGAH to 3PPH and of PGA to 3PP. For every λ point 100 ps of equilibration was followed by 200 ps of data collection. In the transformation an oxygen atom was mutated into a carbon atom and all associated bonded and nonbonded interactions were mutated accordingly. The mass of the atoms was not altered. The integration was carried out numerically using the trapezoidal method. The error in the $\langle \partial H/\partial \lambda \rangle$ was calculated using a block averaging procedure.[26,27] Nonbonded interactions between the initial and the final state were interpolated using a soft-core potential[28] as implemented in the GROMACS package.[21] The soft-core parameter alpha was set to 1.51.

Results and Discussions

The free energy difference between the 2-phosphoglycolic acid and the 3-phosphonopropanoic acid was calculated at different concentrations of ions (Na^+ and Cl^-) in water. The acids are neutral at very low pH (below 2) while they are deprotonated at neutral pH. The transformations were performed on both the neutral (PGAH to 3PPH) and ionic form (PGA to 3PP) of the molecules (Fig. 2). In both cases, the mutation consists of the transformation of a glycolic oxygen atom, Op4, of the 2-phosphoglycolic acid into an aliphatic group, $CH2_b$, of the 3-phosphonopropanoic acid (Fig. 2). The mutation is relatively minor, and involves primarily an atom that is partially buried in the molecule. Moreover, the changes affect only the dipole moment of the solute and do not change the net charge of the system. In Table 2, the free energy differences and corresponding errors are listed for the transformation at different ionic strengths for both the neutral and ionic forms of the compounds. In Figure 3, the $\langle \partial H/\partial \lambda \rangle$ values are shown as a function of λ for the transformations of the neutral and charged systems.

Table 2. Free Energy Difference (in kJ mol^{-1}) for the Transformation of the Neutral (PGAH → 3PPH) and Ionic (PGA → 3PP) Forms of the Inhibitors in Water at Different Ionic Strengths (I) and in Vacuum.

	PGAH → 3PPH	PGA → 3PP	
I	Cutoff 1.4	Cutoff 1.4	Cutoff 1.8
0.0	−81.2 ± 2.4	−109.6 ± 2.7	
0.04	−81.7 ± 2.6	−107.0 ± 9.5	−109.6 ± 6.8
0.06	−82.6 ± 2.6	−112.8 ± 3.8	
0.1	−82.3 ± 2.5	−116.4 ± 10.2	−113.6 ± 8.4
2.0	−82.6 ± 2.7	−127.1 ± 7.6	−132.9 ± 8.9
Vacuum	−67.9 ± 0.8	−91.8 ± 0.8	

Cutoff lengths used to describe electrostatic interactions are indicated in nm. Ionic strength are in M.

In the case of the uncharged compounds, the $\langle \partial H/\partial \lambda \rangle$ profile (Fig. 3a) is smooth and does not change significantly over the range of ionic strength considered. The overall changes in free energy for these transformations are very similar, and show only a slight dependence on the ionic strength. In fact, the values could be considered identical within the limit of the statistical error (Table 2).

The change in free energy associated with the same mutation in the charged species is also presented in Table 2 as a function of ionic strength. Four aspects are evident. First, although the mutation does not involve the creation of charge, the change in free energy is very sensitive to the local charge distribution. Even at zero ionic strength the change in free energy is −110 kJ mol^{-1} in the ionic form compared to only −82 kJ mol^{-1} in the neutral form. Note, this does not translate directly into a difference in free energy, as the reference state for the neutral and charged forms of the inhibitor are different, and thus the values cannot be compared directly. The hydration free energies of the neutral and charged inhibitors can be calculated as the difference in the free energy change for the transformations in water and in vacuum. The free energy differences for the mutations in vacuum are reported in Table 2. The differences in hydration free energy of PGAH-3PPH and PGA-3PP are, respectively, −13 and −18 kJ mol^{-1} at zero ionic strength. However, no experimental data is available for comparison. Second, the calculated free energy is very sensitive to the ionic strength. At the highest ionic strength considered (2 M)

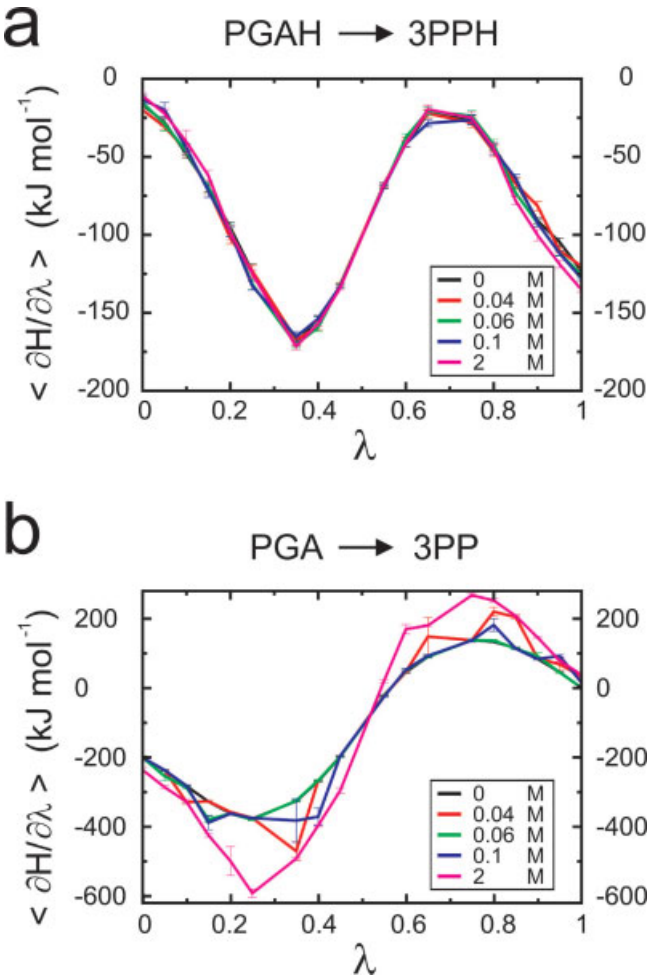

Figure 3. $\langle \partial H/\partial \lambda \rangle$ (in kJ mol^{-1}) as a function of λ for the transformation of PGAH into 3PPH (a) and PGA into 3PP (b) calculated at ionic strengths 0, 0.04, 0.06, 0.1, and 2 M.

the $\langle \partial H/\partial \lambda \rangle$ curve (Fig. 3b) clearly differs from the one obtained in the absence of ions. Third, the inclusion of compensating charges "increases" the magnitude of the free energy differences compared to the neutral form. The free energy difference is about 20 kJ mol^{-1} more negative at an ionic strength of 2 M than at 0 M (Table 2). One might have expected that as the Na^+ ion approached the negatively charged phosphate group the system would more closely approximate the protonated (neutral) form of the compound. In the mutation of PGA to 3PP the positive charge on the P atom decreases (by 0.36 *e*) while the charge on the Op4/$CH2_b$ atom increases by the same amount. The changes are the same in the mutation PGAH to 3PPH. In the ionic form, the mutation would be unfavorable with respect to the negative charges on the phosphoryl oxygen atoms (Op1, Op2, and Op3). These 1–3 interactions are, however, excluded in the calculation and, in fact, make no net contribution to the difference in hydration free energy, as they would be effectively identical in vacuum and solution. The observed difference in free energy derives not from the charge distribution within the molecule itself but from the response of the solvent environment. The negatively charged phosphate oxygens induce a net dipole in the solvent due to the orientation of the surrounding water molecules (dielectric response). The positive end of this dipole is directed toward the solute. This results in the favorable change in free energy associated with the mutation. The approach of a positively charged counterion simply increases the local positive charge making the mutation even more favorable. The fourth aspect that should be noted is that the free energy profiles are very noisy when ions are present (Fig. 3b). The $\partial H/\partial \lambda$ values are poorly converged. The uncertainty in each of the individual values as indicated by the errors in Table 2 is, as a consequence, large, and in fact, only represents an estimate of the minimum statistical error.

To analyze better the effect of ion concentration on the convergence of $\partial H/\partial \lambda$ for the charged form of the inhibitors, the calculations were repeated five times for each λ value at each of the different ionic strengths. Different starting velocities and ion distributions were used for each simulation. To generate new ion distributions the ions were simply placed randomly at a distance of 0.6 nm from the compound. This was done to assure similar, but not identical starting conditions in each case. The value of $\partial H/\partial \lambda$ was again monitored for 200 ps. The results observed at $\lambda = 0.25$ illustrate typical behavior. In absence of ions the $\partial H/\partial \lambda$ was approximately constant in all five simulations. At high ionic strength (2 M), there was a marked jump in the value of $\partial H/\partial \lambda$ of around 200 kJ mol^{-1} within 200 ps in four out of five simulations. At lower ionic strength (0.04, 0.06, and 0.1 M), a similar change is observed only in one out of five simulations. Clearly, when ions are included in the calculations 200 ps is far too short to achieve sufficient sampling to obtain convergence for the PGA–3PP transformation, especially at low ionic strength.

In Figure 4 is shown $\partial H/\partial \lambda$ as a function of time for a 10 ns simulation at $\lambda = 0.80$ of the PGA–3PP transformation at an ionic strength of 0.06 M. The conformations of the inhibitor and the associated ions at four different time frames are also reported. The value of $\partial H/\partial \lambda$ increased by about 200 kJ mol^{-1} at 300 ps and then remained nearly constant during the rest of the simulation. It is clear that the presence of ions around the atoms involved in the mutation has a direct effect on the derivative of the potential respect to λ, and thus on the computed free energy.

To understand better how the distribution of ions in solution affects the free energy, $\partial H/\partial \lambda$ was expressed as a sum of components corresponding to specific bonded and nonbonded interactions. Such a decomposition has little physical meaning as the components are not state functions, but is illustrative in this case.[29,30] Three components were examined: $\partial H/\partial \lambda$ for the Na^+ ions–inhibitor interactions, $\partial H/\partial \lambda$ for the solvent–inhibitor interactions, and $\partial H/\partial \lambda$ for the inhibitor intramolecular interactions. These are plotted for the first 1 ns of the PGA–3PP transformation at an ionic strength of 0.06 M at $\lambda = 0.80$ in Figure 5. The distance of any atom of the charged inhibitor from the closest Na^+ ion is also shown. The presence of a Na^+ ion close to the compound effects not only the Na^+–inhibitor interaction but also the solvent–inhibitor component. The intramolecular component is uneffected by the ion distribution. There is a marked effect of the first ion but the effect of a second or third ion is much smaller (data not shown).

To estimate the residence time of ions around the compound a 60 ns simulation at an ionic strength of 0.1 M (6 Na^+ and 3 Cl^-)

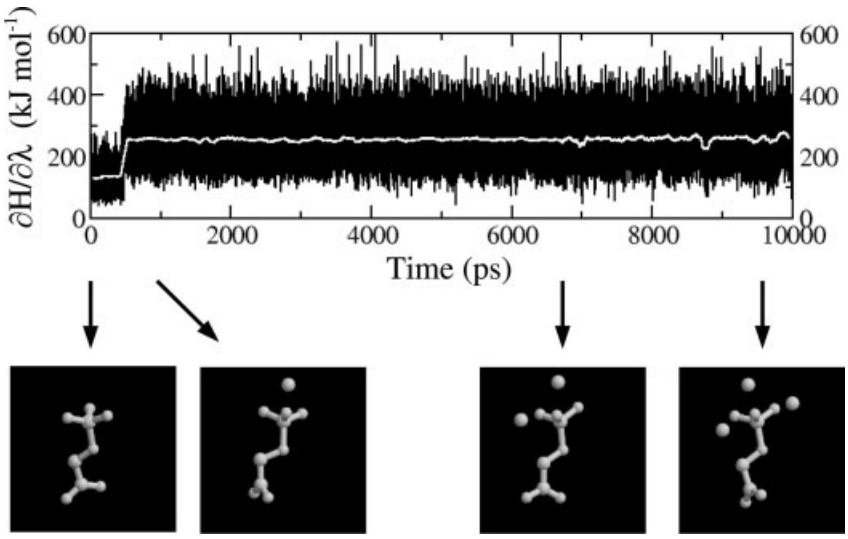

Figure 4. $\partial H/\partial\lambda$ (in kJ mol^{-1}) as a function of time at $\lambda = 0.80$ for the transformation of PGA into 3PP at ionic strength 0.06 M (4 Na^+, 1 Cl^-). The white line in the graph is the average $\partial H/\partial\lambda$ at each 500 ps time window. The conformations of the inhibitor and the Na^+closest ions at four different time frames (0, 0.3, 6.9, 9.6 ns) are shown.

was performed for both the neutral and the deprotonated forms of the 2-phosphoglycolic acid ($\lambda = 0$). An ion (Na^+ or Cl^-) was considered to be in contact with the compound if its distance to any atom of the compound was less than 0.3 nm. In the case of the neutral molecule PGAH (data not shown), ions were rarely found at a distance below 0.3 nm. Ions interacted with PGAH for only approximately 2% of the total simulation time. The average minimum distance between PGAH and the Na^+ ions was 0.95 nm, and between PGAH and the Cl^- ions was 0.97 nm. In contrast, in the 60 ns simulation of the charged PGA in water we observe that there were on average two Na^+ ions at a distance of less than 0.3 nm from the acid (the average minimum distance was 0.22 nm). The ions were mainly found around the phosphate group of the PGA. The minimum distance of each Na^+ ion from the molecule as a function of time is shown in Figure 6. Individual ions spent on

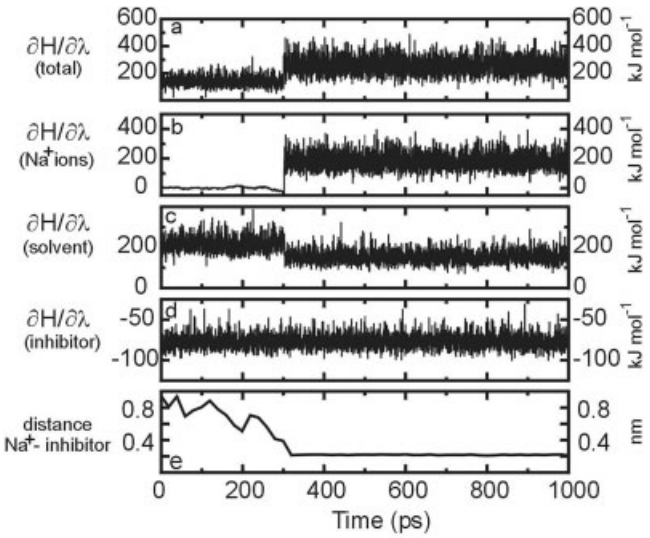

Figure 5. Total $\partial H/\partial\lambda$ (a) and $\partial H/\partial\lambda$ for the Na^+ ions–inhibitor interactions (b), solvent–inhibitor interactions (c) and for the inhibitor intramolecular interactions (d) as function of time (1000 ps) at $\lambda = 0.80$ for the transformation of PGA into 3PP at ionic strength 0.06 M (4 Na^+, 1 Cl^-). The distance (in nm) of any atom of the inhibitor from the closest Na^+ ion as function of time is shown in graph e.

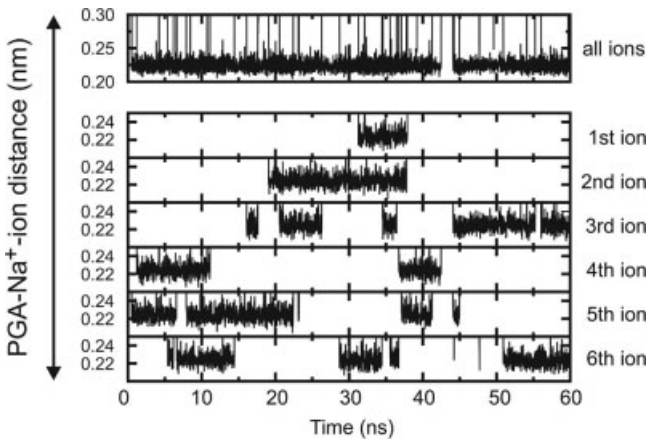

Figure 6. Distance (in nm) as a function of time (60 ns) of Na^+ ions from PGA in solution of ionic strength 0.1 M (6 Na^+, 3 Cl^-). The upper graph shows the distance of all Na^+ ions while in the lower ones each Na^+ ion is shown separately (Na^+ ion first to sixth). The distance is the distance of the ions from the closest atom of the inhibitor. Only distances below 0.3 (multiple ion graph) and 2.5 nm (single ion graphs) are shown.

average 40% of the simulation time at a distance less than 0.3 nm from the acid and exchanged frequently with the average residence time being 6.6 ns. From Figure 6 it can also be seen that between 43 and 44 ns there was no ion close to the inhibitor. This corresponded to about 3% of the total simulation time. During this time the $\partial H/\partial\lambda$ value increased to the value observed in absence of ions (not shown). In contrast to the Na^+ ions, the average minimum distance of the Cl^- ions from PGA was 1.3 nm. The fact that the average residence time of the Na^+ ion was about 7 ns means that very long simulations about 20 to 100 ns at each λ value would be required to obtain convergence when there are small numbers of ions.

During the process of review of this manuscript several important issues regarding this work were raised. In particular, the use of 1.4 nm cutoff, together with a reaction field correction, was questioned. One argument proposed by a reviewer was that the fluctuations in the derivative of the free energy observed would be dominated by the ions entering or leaving the cutoff sphere. This implied that the ion distribution was inappropriate and the results would be very sensitive to the cutoff. The use of an Ewald summation was suggested. Certainly much has been written regarding the relative merits of the use of Ewald summation versus a cutoff with a reaction field. The present study was performed using a cutoff with a reaction field correction, as this approach is commonly used when estimating free energy differences in biological systems. The question of whether the results are dominated by an inappropriate ion distribution close to the cutoff and by ions crossing the cutoff is nevertheless important. In addressing this question we first note that it has been shown previously that ion–ion radial distribution functions for solutions of NaCl in water calculated using a 1.4 nm cutoff plus reaction field or using an Ewald summation are almost identical.[31] This suggests that the ion distributions using a cutoff plus reaction field are reasonable. However, to test the assertion of the reviewer directly, several additional calculations were performed. First, the mutation was performed with cutoff 1.8 nm at three different ionic strengths (0.04, 0.1, and 2 M) to check if the cutoff distance used could be the cause of the instabilities observed in the calculations. The results are reported in Table 2. Increasing the cutoff to 1.8 nm had no significant effect on the free energy difference of the charged inhibitor. The free energy profiles were similar to the ones obtained with a 1.4 nm cutoff (data not shown). This clearly demonstrates that the results are not very sensitive to the precise cutoff. Second, to explicitly check what was the effect of ions crossing the cutoff on the calculated $\partial H/\partial\lambda$, the $\partial H/\partial\lambda$ component of single Na^+ ions were calculated. Figure 7 shows the $\partial H/\partial\lambda$ component together with the ion–solute distance for two representative Na^+ ions. A jump in the value of the $\partial H/\partial\lambda$ component (about 200 kJ mol^{-1}) is observed when the ion approaches very close to the inhibitor (Fig. 7b). The crossing of the cutoff by the ions has, in contrast, only a small effect on $\partial H/\partial\lambda$ values. Again, it appears that reaction field effectively minimizes any potential cutoff effects and any noise due to ions crossing the cutoff is of minor importance. Third, to test if there were any significant differences in the ion distribution or lifetimes a 60 ns simulation of PGA in water at ionic strength 0.06 M was performed using the particle mesh Ewald (PME) method to describe the long-range electrostatics. There were, on average, 2 Na^+ ions at a distance of less than 0.3 nm from PGA (the average minimum distance was 0.22 nm) as observed in the simulation with 1.4 nm cutoff. Individual ions spent on average 39% (against 40% using 1.4 nm cutoff) of the simulation time at a distance less than 0.3 nm from the acid and

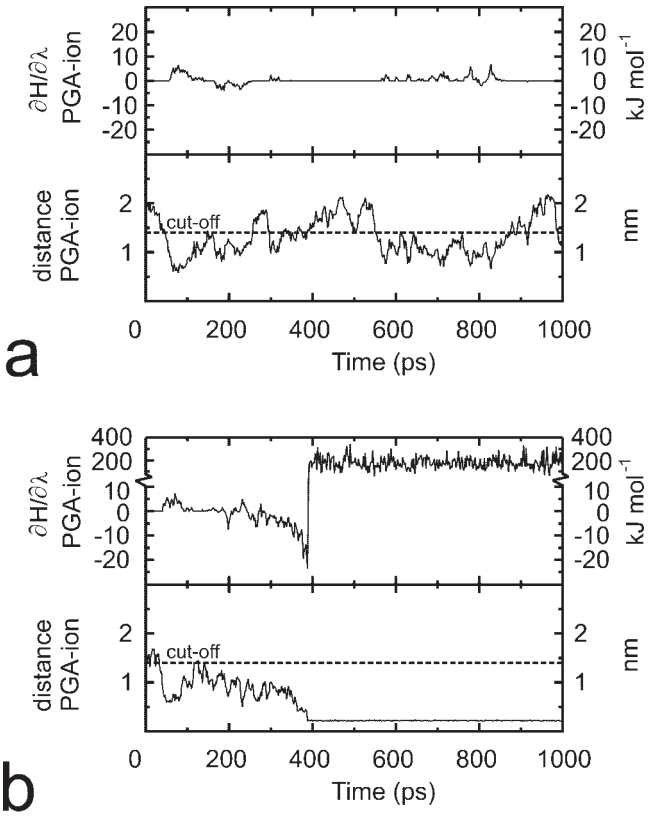

Figure 7. $\partial H/\partial\lambda$ component for the Na^+ ion–inhibitor interactions (upper graph) and ion–inhibitor distance (lower graph) as function of time for two Na^+ ions, in (a) and (b), respectively. Calculations are performed at $\lambda = 0.80$ for the transformation of PGA into 3PP at ionic strength 0.06 M (4 Na^+, 1 Cl^-). The distance is the distance of the ion from the closest atom of the inhibitor. Note a different scale was used for the $\partial H/\partial\lambda$ component in (a) and (b). The dashed line indicates the cutoff distance at 1.4 nm.

exchanged frequently with the average residence time being 6.0 ns (against 6.6 ns using 1.4 nm cutoff). As concluded using 1.4 nm cutoff, long simulations (20–100 ns) are needed to obtain convergence when a small number of ions are present in solution. Clearly, any differences are negligible.

There is one final aspect of this discussion that must also be addressed. In the simulation community there is growing tendency to assume that results obtained using the Ewald summation are necessarily to be preferred. Some of the comments related to the original version of this manuscript reflect this. In regard to free energy calculations involving the creation or deletion of charge this is far from certain.[32] Lattice sum techniques in general require that the basic unit cell is neutral. In an Ewald summation a background charge is added to compensate for any net charge on the system. During a free energy calculation work will be done against this background charge. In most implementations including that of GROMACS the background charge is uniform across the simulation box. This, however, obviously bears little relationship to a true counterion distribution and thus the calculated free energy is likely to be inappropriate.

Conclusions

To investigate the effect of the inclusion of explicit ions in free energy calculations the free energy difference between two TIM inhibitors, 2-phosphoglycolic acid and 3-phosphonopropanoic acid, was calculated in water solution at five ionic strengths using TI and MD simulations. The calculations were performed using the neutral and charged forms of the compounds. When the transformation involved the neutral species the effect of the ion concentration on the free energy difference was small. In contrast, when the mutation involved the charged species, the presence of counterions close to the solute affected the computed free energy differences significantly. The free energy values differed by up to 20 kJ mol^{-1} between 0 and 2 M ionic strength despite the mutation itself not involving a change in net charge. Experimentally, changes in the ionic strength are known to effect thermodynamic properties of a system such as binding affinities by as much as a few kJ mol^{-1} for a twofold increase in ionic strength.

The work has demonstrated that the influence of the distribution of ions around the compound cannot be ignored even for mutations that do not involve a change in the net charge. Moreover, the precise position of the ions is more important than the number of ions. This meant that when only a small number of counterions were included in the system there were large fluctuations in $\partial H/\partial\lambda$, and very long simulation times were required to obtain convergence.

Experimentally, the effect of the ionic strength on free energy differences is not expected to be very large. Usually it will fall within the error limits of a free energy calculation. Thus, although differences in the calculated free energy can already be observed when only a few counterions are included to neutralize the charge of the solute, the effect, when averaged over all possible distributions, is not large. In practice, to obtain converged results it is better to either (a) perform the calculation without including counterions and rely on the dielectric response of the solvent to induce an opposing local charge distribution even if this does mean the total system has a net charge, or (b) to include many ions and perform the calculation at high ionic strength to ensure sufficient averaging. If only sufficient ions to ensure overall neutrality of the system are included, very long simulation times will, in general, be required or else the calculated free energy will be heavily dependent on the initial distribution of ions.

Acknowledgments

The authors thank Gerrit Groenhof of the University of Groningen (The Netherlands) for his assistance in the implementation of required modifications in GROMACS.

References

1. Beveridge, D. L.; DiCapua, F. M. Annu Rev Biophys Biophys Chem 1989, 18, 431.
2. Kollman, P. A. Chem Rev 1993, 93, 2395.
3. Mark, A. E. In Encyclopedia of Computational Chemistry; von Rague Schleyer, P., Ed.; John Wiley & Sons: New York, 1998, p. 1070, Vol. 2.
4. van Gunsteren, W. F.; Daura, X.; Mark, A. E. Helv Chim Acta 2002, 85, 3113.
5. Wang, W.; Donini, O.; Reyes, C. M.; Kollman, P. A. Annu Rev Biophys Biomol Struct 2001, 30, 211.
6. Lambeir, A. M.; Opperdoes, F. R.; Wierenga, R. K. Biochemistry 1987, 168, 69.
7. Fedosova, N. U.; Champeil, P.; Esmann, M. Biochemistry 2002, 41, 1267.
8. Goto, Y.; Fink, A. L. J Mol Biol 1990, 214, 803.
9. Rao, B. G.; Tilton, R. F.; Singh, U. C. J Am Chem Soc 1992, 114, 4447.
10. Dixit, S. B.; Chipot, C. J Phys Chem A 2001, 105, 9795.
11. Donnini, S.; Juffer, A. H. J Comp Chem 2004, 25, 393.
12. Noble, M. E. M.; Wierenga, R. K.; Lambeir, A. M.; Opperdoes, F. R.; Thunnissen, A. M. W. H.; Kalk, K. H.; Groendijk, H.; Hol, W. G. J. Proteins Struct Funct Genet 1991, 10, 50.
13. Lolis, E.; Petsko, G. A. Biochemistry 1990, 29, 6619.
14. Kursula, I.; Wierenga, R. K. J Biol Chem 2003, 278, 9544.
15. van Gunsteren, W. F.; Billeter, S. R.; Eising, A. A.; Hünenberger, P. H.; Krüger, P.; Mark, A. E.; Scott, W. R. P.; Tironi, I. G. Biomolecular Simulation: GROMOS96 Manual and User Guide. Vdf Hochschulverlag AG an der ETH. Zürich, 1996.
16. http://www.gromacs.org/contributions ffG43a1p: uploaded 16:08 May 15, 2002 by Graham Smith.
17. Hansson, T.; Nordlund, P.; Åqvist, J. A. J Mol Biol 1997, 265, 118.
18. Frisch, M. J.; Trucks, G. W.; Schlegel, H. B.; Gill, P. M. W.; Johnson, B. G.; Robb, M. A.; Cheeseman, J. R.; Keith, T. A.; Petersson, G. A.; Montgomery, J. A.; Raghavachari, K.; Al-Laham, M. A.; Zakrzewski, V. G.; Ortiz, J. V.; Foresman, J. B.; Ciosloswki, J.; Stefanof, B. B.; Nanayakkara, A.; Challacombe, M.; Peng, C. Y.; Ayala, P. Y.; Chen, W.; Wong, M. W.; Andres, J. L.; Replogle, E. S.; Gomperts, R.; Martin, R. L.; Fox, D. J.; Binkley, J. S.; Defrees, D. J.; Baker, J.; Stewart, J. P.; Head–Gordon, M.; Gonzalez, C.; Pople, J. A. Gaussian 94, revision A.1; Gaussian, Inc.: Pittsburgh, PA, 1995.
19. Berendsen, H. J. C.; van der Spoel, D.; van Drunen, R. Comp Phys Commun 1995, 91, 43.
20. van der Spoel, D.; van Buuren, A. R.; Apol, E.; Meulenhoff, P. J.; Tieleman, D. P.; Sijbers, A. L. T. M.; Hess, B.; Feenstra, K. A.; Lindahl, E.; van Drunen, R.; Berendsen, H. J. C. Gromacs User Manual Version 3.1. Nijenborgh 4, 9747 AG: Groningen, The Netherlands (Internet: http://www.gromacs.org, 2002).
21. Lindahl, E.; Hess, B.; van der Spoel, D. J Mol Model 2001, 7, 306.
22. Berendsen, H. J. C.; Postma, J. P. M.; van Gunsteren, W. F.; Hermans, J. In Intermolecular Forces; Pullman, B., Ed.: Reidel: Dordrecht, 1981, p. 331.
23. Berendsen, H. J. C.; Postma, J. P. M.; van Gunsteren, W. F.; DiNola, A.; Haak, J. R. J Chem Phys 1984, 81, 3684.
24. Miyamoto, S.; Kollman, P. A. J Comp Chem 1992, 13, 952.
25. Hess, B.; Bekker, H.; Berendsen, H. J. C.; Fraaije, J. G. E. M. J Comp Chem 1997, 18, 1463.
26. Allen, M. P.; Tildesley, D. J. Computer Simulation of Liquids: Oxford Science Publication: Oxford, 1987.
27. Hess, B. J Chem Phys 2002, 116, 209.
28. Buetler, T. C.; Mark, A. E.; van Schaik, R. C.; Geber, P. R.; van Gunsteren, W. F. Chem Phys Lett 1994, 222, 529.
29. Smith, P. E.; van Gunsteren, W. F. J Phys Chem 1994, 98, 13735.
30. Mark, A. E.; van Gunsteren, W. F. J Mol Biol 1994, 240, 167.
31. Tironi, I. G.; Sperb, R.; Smith, P. E.; van Gunsteren, W. F. J Chem Phys 1995, 102, 5451.
32. Hünenberger, P. H.; McCammon, J. A. J Chem Phys 1999, 110, 1856.